JOURNAL OF UNDERGRADUATE RESEARCH

Assessing the Validity of Ultrasound Imaging of Wrist Muscle Moment Arms through an Agar Phantom Experiment and *In Vivo* Case Study

Jonathan P. Charles, & Jennifer A. Nichols
University of Florida

Faculty Mentor: Jennifer A. Nichols, Department of Biochemical Engineering

Abstract

Joints in the human body utilize torque to create movement, where a force, **F,** acts at a distance, **r,** from a rotation point. In biomechanics, **F** is generated by muscles acting on the joint, and **r** is the distance between the joint's center of rotation (COR) and the muscle line of action. This distance **r** is known as a geometric moment arm (GMA). Changes in GMAs may be correlated with loss of muscle and hand function in people due to aging, injury, or pathology. To comprehensively evaluate GMAs, efficient and inexpensive methods for measuring them *in vivo* are needed. Thus, this study explores whether ultrasound is a valid imaging modality for quantifying the GMA of muscles crossing the wrist. An agar-gel phantom was used to determine if distance measurements from 20 ultrasound images of the phantom were accurate compared to a set of four baseline distances. A subsequent *in vivo* case study explored whether ultrasound could measure GMAs within a human wrist. The capitate bone was defined as the wrist's COR due to its central location in the joint, and the measured GMA was defined between this COR and the *flexor digitorum superficialis* (FDS) muscle. Both studies returned data that exhibited low measurement variability over consecutive days and provided reasonable proof that ultrasound can accurately measure wrist GMAs.

Keywords: biomechanics, medical imaging, capitate, flexor digitorum superficialis

Introduction

Joints in the human body can be represented by simple machines, utilizing properties such as mechanical advantage, work, and torque. Importantly, torque (**τ**) is defined as the twisting force associated with an object, or mathematically, as the cross product of a force (**F**), and the perpendicular distance between the line of action of force and the axis of rotation of the object, (**r**):

$$\boldsymbol{\tau} = \mathbf{r} \times \mathbf{F} \tag{1}$$

Anatomical joints utilize this fact to create movement, where **F** is created by muscles and tendons surrounding a joint, and **r** is the physical distance between the joint COR and the muscle-tendon line of action. In biomechanics, **r** is known as the geometric moment arm (GMA). GMAs transform muscle forces into joint torque, enabling movement.

A major challenge in measuring GMAs is the difficulty associated with directly visualizing them. To date, studies examining lower-extremity GMAs in the hip (Fontana *et al.*, 2020; Visser *et al.*, 1990), knee (Spoor *et al.*, 1990; Visser *et al.*, 1990), and ankle (Adamcyzk, 2019; Spoor *et al.*, 1990) far outnumber those studying upper-extremity GMAs. The disparity in the amount of literature between upper- and lower-extremity GMAs may be due to the complexity associated with upper-extremities. This does not imply that work has not been conducted to better conceptualize the wrist, but rather that this imbalance is problematic for fully understanding the upper-extremities. For example, use of magnetic resonance imaging (MRI) comparing *in vivo* and *in vitro* measurements of wrist GMAs (Garland *et al.*, 2018; Loren & Lieber, 1995) has furthered our understanding of wrist GMAs, moving the field closer to the creation of subject-specific computer models of the wrist. However, there are scant studies using MRI or other imaging methods to quantify upper extremity GMAs *in vivo.*

There is an unmet need for clinicians and researchers to have an imaging system that enables measurement of wrist GMAs in real-time, without the lengthy procedure required for MRI imaging. With such a system, a promising end-objective would be the creation of a comprehensive, subject-specific model illustrating a subject’s individual joint architecture and GMAs. This model could allow clinicians and researchers to tailor their approach to individual patients, producing more effective results. Medical practitioners could, in the future, measure a patient’s GMA and determine if they are achieving optimal levels of hand function based on their torque generation. Researchers could efficiently explore questions regarding how GMAs change with age, injury, or pathology.

To successfully build this model, two overarching components are required: (1) a large number of subjects from which to build a data-base of muscle properties, and (2) relative ease in imaging subjects. Requiring MRI is unreasonable due to high costs and substantial time required to complete the procedure. Measuring cadaveric GMAs is not logistically feasible for a demographically diverse dataset requiring hundreds of subjects. In contrast, ultrasound may hold the key for achieving high-resolution imaging of the wrist in a fast and cost-effective manner.

The objective of this study is to determine if ultrasound can accurately measure wrist GMAs. An agar-gel phantom, which has been shown to mimic tissue's acoustic properties (Chen & Balter *et al.* 2016; Earle *et al.* 2016; Menikou & Damianou 2017; Zell *et al.* 2007), was used to test whether standard B-mode ultrasound can reliably measure distances similar to wrist GMAs. It was hypothesized that the phantom study would provide accurate results due to the reliability of ultrasound in other disciplines (Gerganov *et. al.*, 2009). As an integral step toward demonstrating to what extent ultrasound can successfully image human wrist architecture, a case study was performed.

Methods

This study aims to determine the validity of ultrasound in imaging human wrist GMAs. Metal rods placed within an agar-gel phantom and the GMA of the *flexor digitorum superficialis* (FDS) were imaged and measured using standard B-mode ultrasound (L18-5 linear transducer; Supersonic Imaging Aixplorer Mach-30). Images were acquired over three consecutive days for the phantom, and over five consecutive days for the case study. GMAs were measured with the machine's built in linear-measurement tool, which can resolve 0.1mm distances.

Agar-gel Phantom

An agar-gel phantom study determined the validity of the ultrasound machine's measurement system. Agar-gel was used for its similar acoustic properties to human tissue.

phantom construction. The agar-gel phantom was built using a protocol that bypasses the need for refrigeration (Earle *et al.*, 2016). Briefly, the agar-gel phantom was composed of 5% dry agar flakes and 95% deionized water, by mass. To dissolve the agar flakes, a 1L solution was heated at 325F and stirred at a rate of 50 RPM using a magnetic stir bar (approximately 45 minutes). Once dissolved, the solution was poured into a rectangular glass container and cooled at room temperature.

Muscles were simulated in the phantom with metal rods. To replicate distances on the scale of the human wrist (Erwin & Varacallo, 2018), five, 100mm-long, 1mm-diameter metal rods were suspended in parallel within the agar (Figure 1). To suspend the rods, a bilayer agar-gel phantom methodology was devised. Specifically, the protocol described previously was performed twice. The first agar-gel layer filled the glass container half-way and was allowed to solidify. Then, five "slits" were made in parallel superficially on the first layer and each metal rod was inserted into a "slit". Baseline distances between each "slit" (22.754mm, 16.744mm, 13.434mm, 5.948mm) were chosen with the goal of assessing distances within the range of 5mm – 25mm (range of wrist GMAs reported previously)) (Loren & Leiber 1995; Brand & Hollister, 1999; Crisco *et al.*, 2005, Garland *et. al.*, 2018). Electronic calipers were used to measure the baseline distances. The second half of the agar-gel solution was then prepared, poured over the first layer and metal rods, and allowed to solidify.

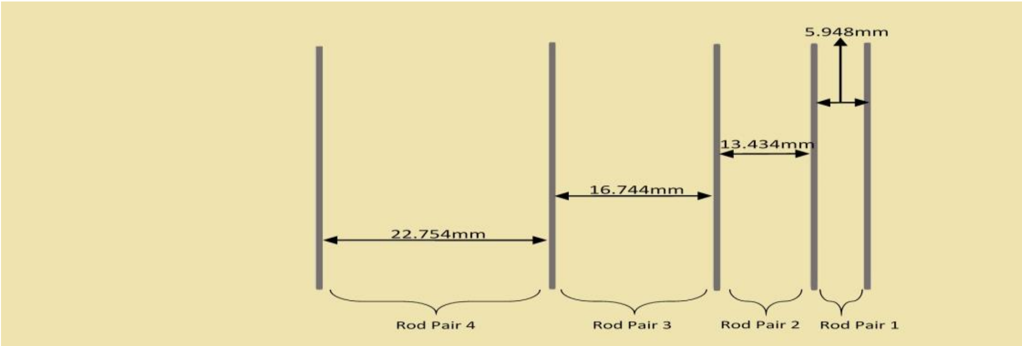

Figure 1. Agar-gel phantom top-down schematic with rod pairs and separations outlined.

measurement. Over three days, the baseline distances for each rod pair were transversely imaged with a linear ultrasound transducer. Images were acquired five times per day. A total of 20 measurements were taken across all four metal rod pairs each day. All images were recorded by a single sonographer with the same ultrasound machine, transducer, phantom, and settings (Table 1). Each imaging session lasted approximately 15 minutes.

Table 1. SuperSonic Imagine Aixplorer Mach-30 Image Acquisition Settings

Component	Setting	Meaning
Linear Transducer	L18-5 / MSK / WRIST TENDON	The transducer used, optimized for imaging the wrist
Optimization	Penetration	Focuses the ultrasound waves to achieve a greater depth
TissueTuner™	1540 m/s	The speed of the sound waves (optimized for live tissue)
Dynamic Range	50dB	Adjusting the echo intensity
2D Map	1	A color map of the image
Sector Size	Large	Width and Depth of the image
Brightness (G)	45%	How bright the image will be
Zoom	120%	The magnification of the image

The distances in each image were measured in centimeters utilizing the ultrasound machine's built-in linear measurement tool. Briefly, for the measurement, the sonographer would capture an image, activate the measurement tool, and dynamically select two points in the image. The distance between the points was then calculated automatically based on pixel size (Figure 2).

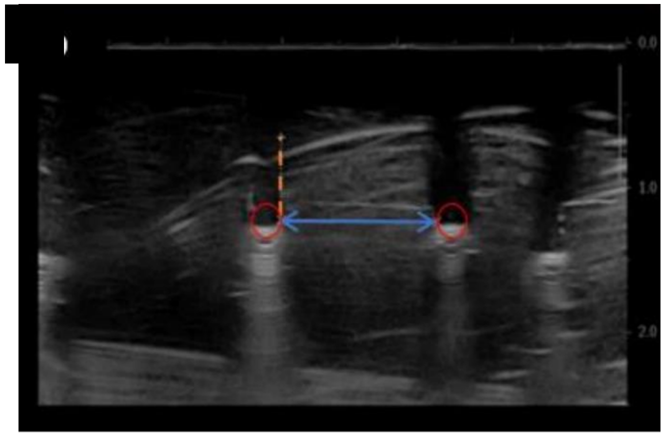

Figure 2 - Ultrasound image of a metal rod pair. The rods (red) are some distance (blue) apart. This distance was measured by the sonographer with the software.

analysis. To test the precision of the software, and the variability of the measurements over time, averages were calculated for each day and metal rod pair. Percent error between the baseline distances and measured averages were calculated for each day and rod pair, and plotted. A one-way ANOVA and multiple comparisons using a Tukey post hoc test (alpha = 0.05) were conducted to determine if any of the daily means were significantly different.

***In Vivo* Case Study**

This case study examines whether ultrasound imaging can be used in humans to measure the GMAs between the wrist joint COR and muscle-tendon lines of action. In this IRB approved study (University of Florida, IRB #201802358) the right wrist of one subject (male, age 22) was longitudinally imaged over the course of five consecutive days. A water bath technique (Blaivas *et al*., 2004) was utilized for the decreased soundwave attenuation in water compared to air, producing a clearer image. The capitate wrist bone (Figure 3) was chosen as the joint COR for its central location within the wrist, ease of identification when imaging, and use in prior work (Andrews & Youm, 1979).

Figure 3 - Dorsal view of a human right hand. The capitate wrist bone is highlighted in red. [Adapted from BodyParts3D by DBCLS]

measurement. The shortest distance between the surface of the capitate and the FDS was measured using the ultrasound machine's measurement tool. The FDS was chosen for its close proximity to the capitate and ease of identification. The sonographer followed the steps outlined in Agar-gel Phantom for the machine settings and image acquisition. The subject's right wrist was submerged in room temperature water. Over five consecutive days, a total of 25 images were acquired by taking five longitudinal images of the capitate and FDS each day (Figure 4). The linear distance between the capitate's palmar surface and FDS was measured for each image.

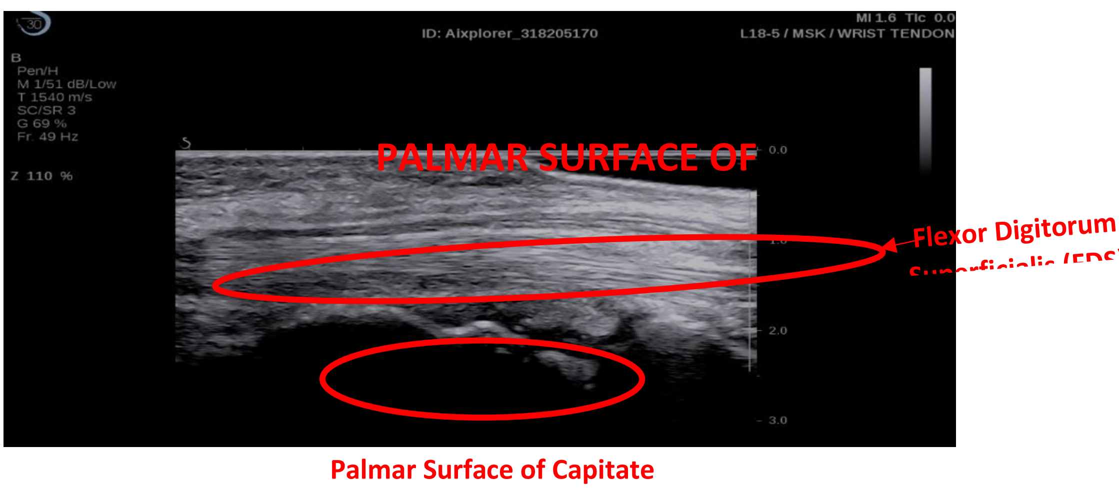

Figure 4 - Ultrasound image of the palmar surface of the capitate and the FDS.

calculating the wrist joint COR. Recall, a GMA is the shortest distance between the joint's COR and the muscle-tendon line of action. The wrist's COR was assumed to be coincident with the center of the capitate. This location was determined from three measurements (Figure 5): (1) the width of the subject's right hand at the location of the capitate, (2) the distance between the palmar surface of the capitate and the palmar surface of the right hand, and (3) the distance between the dorsal surface of the capitate and the dorsal surface of the right hand. Subtracting the sum of (2) and (3) from (1) gives the width of the capitate bone itself. Dividing this value in half provides an estimation of the physical center of the capitate. This final value was added onto each of the 25 measurement values, thus approximating the GMA between the COR of the capitate and FDS.

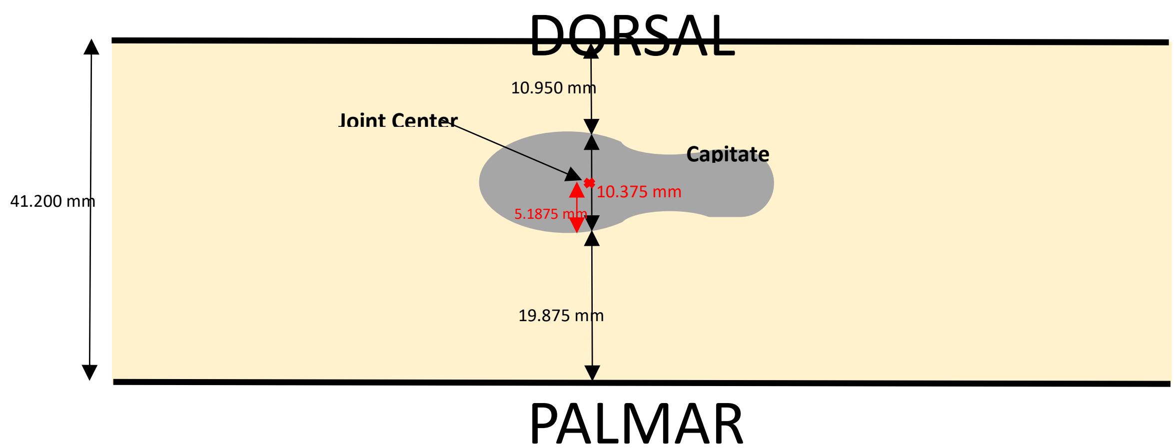

Figure 5 - Visual representation of the capitate COR calculation.

analysis. After calculating the GMA of the FDS in all 25 images, an average of the measurements from each day was calculated. An overall average was taken of all 25 measurements and daily standard deviations were computed to evaluate measurement error. The daily averages and respective standard deviations were plotted. A one-way ANOVA test and multiple comparisons using a Tukey post hoc test (alpha = 0.05) were conducted to determine if measurements were significantly different across days.

Results

Agar-gel Phantom

In the agar-gel phantom study, across the typical magnitude of wrist GMAs (10mm – 20mm), the error between measurements quantified from the ultrasound images and the caliper baseline did not exceed 5%. This indicates that the errors were no larger than 0.5mm – 1.0mm. It should be noted that the errors did tend to increase from the first day of recording to the last (c.f., Figure 6, increasing spread of error bars from the blue bars to the yellow bars for each metal rod pair).

The one-way ANOVA (alpha = 0.05) showed a statistically significant difference between the means over the three days. A Tukey post hoc test revealed that the measurements of metal rod pair 3 (separation distance of 16.744mm) were significantly different ($p = 0.05$) over the three recording days.

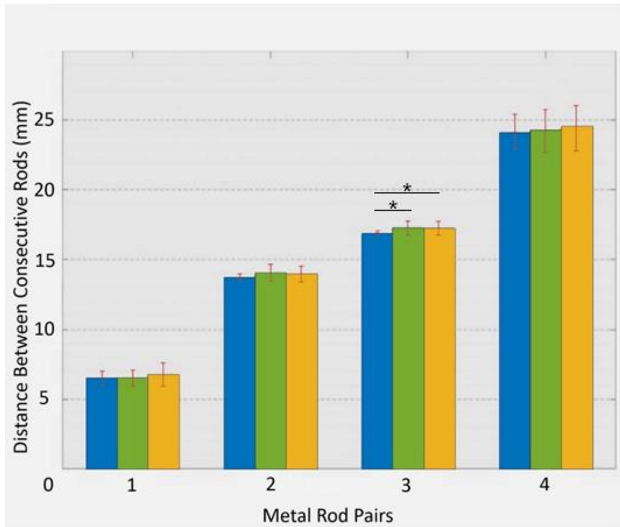

Figure 6 - Averages (millimeters, mean ± % error) from the phantom study for each metal rod pair. Colors represent different recording days: Monday (blue), Wednesday (green), Friday (yellow).
Asterisks (*) indicates statistically significant difference in means

In Vivo Case Study

In the *in vivo* case study, across each of the days, the measurement means stayed relatively constant around a value of 1.6 ± 0.3 cm (Figure 10). The daily standard deviations calculated from the overall GMA measurement mean were small (≤ 0.056cm). The largest standard deviation occurred on Tuesday, with the smallest on Friday. There were no discernable trends to the changes in means and standard deviations across the five days. A one-way ANOVA test (alpha = 0.05) indicated that there was no statistically significant difference ($F = 1.24$, $p = 0.32$) in measurement means between each day of recording.

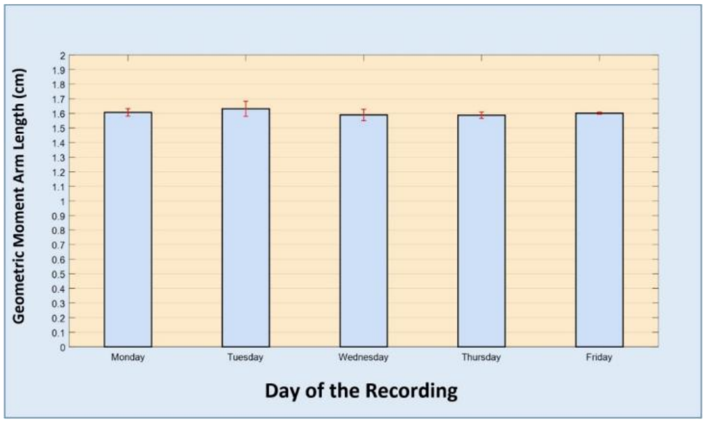

Figure 10 – Av (centimeters, mean ± std. dev.) from the in vivo case study for each day over the five consecutive days, Monday through Friday.

Discussion

The agar-gel phantom study demonstrated that for distances similar to those in the wrist, ultrasound is an effective method to obtain images and accurately measure distances, independent of time of recording. Through the case study, it was demonstrated that ultrasound can reliably image the wrist GMAs *in vivo*, also independent of time of recording.

The agar-gel phantom study indicated that the error associated with the built-in measurement tool is acceptable for imaging the human wrist with ultrasound. Notably, the observed 5% error translates into a physical error of approximately 0.5mm – 1.0mm. On the scale of the human wrist, approximately 30mm – 40mm (Crisco *et al.*, 2005), this error can be assumed to be negligible. When this error is examined in terms of torque production about CORs in the wrist, a 0.5mm – 1.0mm change in GMA length provides a negligible change in the torque output required during activities of daily living. For example, given a force, **F = 0.98N** (the force required to lift 100grams against gravity) that is acting at a 90º angle to the lever arm, **r**, the torque vector, $\boldsymbol{\tau}$ will be 0.00049N·m for **r = 0.5mm**, and 0.00098N·m for **r = 1.0mm.** The torque required to turn a circular doorknob is 0.346N·m (DesignDecisions, 2007). Thus, the change in **r,** or rather the change in GMA, translates to a 0.14% - 0.28% change in the torque required to turn a doorknob.

Although the errors were small, they increased from the first day of recording through the last. Though this could be attributed to some flaw in the ultrasound machine's functioning, it is unlikely as the intra-day measurements did not exhibit significant variability. In other words, the machine was returning daily measurements that were consistent, but each subsequent day was slightly more inconsistent with the baseline distances. A reason for this phenomenon is the material properties of the phantom. Though a durable material, agar-gel is subject to degradation from handling and usage. The surface of the phantom was continually scanned with the transducer, which was in physical contact with the phantom to achieve a clear image. The force between transducer and phantom may have caused the metal rods within the gel to drift from their initial positions over time. This suggests that the rods were no longer at the initial distances. Though the individual measurements were recorded from the drifted positions of the rods, the errors were still calculated from the baseline measurements initially set. Future studies utilizing agar-gel phantoms should take this property into consideration.

The *in vivo* study found that the FDS GMAs were close to a value of 1.6 ± 0.3 cm. This is similar to Brand & Hollister, who measured the GMA of the third compartment of the FDS in 11 cadaveric hands using tendon excursion and reported an average length of ~1.50 cm (Brand & Hollister 1999). The magnitude of the measured FDS GMA is also supported by literature on nearby wrist muscles. For example, Gonzalez et. al. (1997) measured the GMAs in flexion-extension (FE) for several wrist muscles. Two of which, the *flexor carpi radialis* (FCR) and the *flexor carpi ulnaris* (FCU), lie adjacent to the FDS tendon. They found that the FCR had an average GMA of 1.55cm, while the FCU had an average GMA of 1.30cm (Gonzalez *et al.,* 1997). Similarly, Garland et al. (2018) measured wrist GMAs with scaled-MRI and tendon excursion methods between the capitate and various muscles, including the FCR and FCU. They found that the FCU had a scaled MRI-measured GMA of 1.31 ± 0.22 cm and a tendon excursion-measured GMA of 1.13 ± 0.21 cm , and the FCR had a scaled MRI-measured GMA of 1.66 ± 0.28 cm and tendon excursion-measured GMA of 1.22 ± 0.21 cm (Garland *et al.,* 2018). Both studies showed a high degree of correspondence between the FDS and FCR GMA measurements, while detailing a lower degree between the FDS and FCU. This similarity can be attributed to the proximity of the FCR and FCU to the FDS, with the former positioned closer in anatomical space.

Concerning this study, the error was presented as standard deviations calculated from the measurements over the five days. Across the days, measurement errors were small, with the largest on the second day and the smallest on the last day. These values demonstrated that the daily measurements were similar to the average of the entire data set and were consistent throughout the recording period. The one-way ANOVA test reinforced this point, as it showed that there was no statistically significant difference in the daily means between each day. In essence, no matter the day of the recording, the results indicated that the ultrasound machine will capture a consistent image and measure a consistent value.

The water bath technique proved to be much better in maintaining image clarity versus dry-skin or lubricant-assisted imaging. The soundwave attenuation in water is greatly reduced when compared to that in air due to the increased density of water (Francois & Garrison, 1982). This provides for a better image because a greater magnitude of soundwaves emitted by the transducer are able to reach and reflect off the target back to the transducer. It was noted that image quality was best when the transducer was held perpendicular to the surface being imaged and scanned the surface at a slow yet constant rate.

Overall, this work lays the groundwork for ultrasound to quantify GMAs in the wrist. It was demonstrated that ultrasound is viable under controlled conditions where the GMAs of one muscle were measured. Future work that provides measurements for all GMAs within the wrist must be conducted to conclude that ultrasound is a viable method for imaging wrist GMAs, and to begin building a comprehensive, subject-specific musculoskeletal model. Another avenue of future work is development of novel ultrasound imaging techniques. To individually image and measure each GMA can be tedious due to the large number of joint/tendon pairs in the wrist. Imaging techniques that capture multiple pairs simultaneously is crucial for moving forward. Future work could also assess whether changes in wrist GMA magnitude occur with age, injury, and pathology.

References

Adamczyk, P. G. (2019). Ankle Control in Walking and Running: Speed- and Gait-related Changes in Dynamic Mean Ankle Moment Arm (DMAMA). *Journal of Biomechanical Engineering*. doi: 10.1115/1.4045817

Andrews, J., & Youm, Y. (1979). A biomechanical investigation of wrist kinematics. *Journal of Biomechanics*, *12*(1), 83–93. doi: 10.1016/0021-9290(79)90012-5

Blaivas, M., Lyon, M., Brannam, L., Duggal, S., & Sierzenski, P. (2004). Water bath evaluation technique for emergency ultrasound of painful superficial structures. *The American Journal of Emergency Medicine*, *22*(7), 589–593. doi: 10.1016/j.ajem.2004.09.009

Brand, P. W., & Hollister, A. M. (1999). *Clinical mechanics of the hand* (3rd ed.). St. Louis, Mo: Mosby.

Chen, A. I., & Balter, M. L. (2016). Multilayered tissue mimicking skin and vessel phantoms with tunable mechanical, optical, and acoustic properties. *Medical Physics*, *43*(6), 3117–3131. doi: 10.1118/1.4951729

Crisco, J. J., Coburn, J. C., Moore, D. C., & Upal, M. A. (2005). Carpal bone size and scaling in men versus in women. *The Journal of Hand Surgery*, *30*(1), 35–42. doi: 10.1016/j.jhsa.2004.08.012

DesignDecisions. (2007). Babyproof door knob lock. Retrieved from https://wiki.ece.cmu.edu/ddl/index.php/Babyproof_door_knob_lock

Earle, M., Portu, G. D., & Devos, E. (2016). Agar ultrasound phantoms for low-cost training without refrigeration. *African Journal of Emergency Medicine*, *6*(1), 18–23. doi: 10.1016/j.afjem.2015.09.003

Erwin, J. & Varacallo, M. Anatomy, Shoulder and Upper Limb, Wrist Joint. (2018). *StatPearls*. StatPearls Publishing; 2020. https://www.ncbi.nlm.nih.gov/books/NBK534779/

Fontana, H. D. B., Campos, D. D., Sawatsky, A., Han, S.-W., & Herzog, W. (2019). Why do muscles lose torque potential when activated within their agonistic group? *The Journal of Experimental Biology*, *223*(1). doi: 10.1242/jeb.213843

Francois, R.E. & Garrison, G.R. (1982). Sound absorption based on ocean measurements. Part II: Boric acid contribution and equation for total absorption. *Journal of the Acoustical Society of America*, 72, 1879–1890. doi: 10.1121/1.388673.

Garland, A. K., Shah, D. S., & Kedgley, A. E. (2018). Wrist tendon moment arms: Quantification by imaging and experimental techniques. *Journal of Biomechanics*, *68*, 136–140. doi: 10.1016/j.jbiomech.2017.12.024

Gerganov, V. M., Samii, A., Akbarian, A., Stieglitz, L., Samii, M., & Fahlbusch, R. (2009). Reliability of intraoperative high-resolution 2D ultrasound as an alternative to high–field strength MR imaging for tumor resection control: A prospective comparative study. *Journal of Neurosurgery*, *111*(3), 512-519. doi:10.3171/2009.2.jns08535

Gonzalez, R. V., Buchanan, T. S., & Delp, S. L. (1997). How muscle architecture and moment arms affect wrist flexion-extension moments. *Journal of Biomechanics*, *30*(7), 705–712. doi: 10.1016/s0021-9290(97)00015-8

Loren, G. J., & Lieber, R. L. (1995). Tendon biomechanical properties enhance human wrist muscle specialization. *Journal of Biomechanics*, *28*(7), 791–799. doi: 10.1016/0021-9290(94)00137-s

Menikou, G., & Damianou, C. (2017). Acoustic and thermal characterization of agar based phantoms used for evaluating focused ultrasound exposures. *Journal of Therapeutic Ultrasound*, *5*(1). doi: 10.1186/s40349-017-0093-z

Spoor, C.W., van Leeuwen, J.L., Meskers, C.G., Titulaer, A. F., & Huson, A. (1990). Estimation of instantaneous moment arms of lower-leg muscles. *Journal of Biomechanics*, *23*(12), 1247 – 1259. doi : 10.1016/0021-9290(90)90382-d

Visser, J. J., Hoogkamer, J. E., Bobbert, M. F., & Huijing, P. A. (1990). Length and moment arm of human leg muscles as a function of knee and hip-joint angles. *European Journal of Applied Physiology and Occupational Physiology*, *61*(5-6), 453–460. doi: 10.1007/bf00236067

Zell, K., Sperl, J. I., Vogel, M. W., Niessner, R., & Haisch, C. (2007). Acoustical properties of selected tissue phantom materials for ultrasound imaging. *Physics in Medicine and Biology*, *52*(20). doi: 10.1088/0031-9155/52/20/n02